Available online at www.sciencedirect.com
SCIENCE DIRECT
Polymer 46 (2005) 9725–9735
polymer
www.elsevier.com/locate/polymer

Synthesis and characterization of a series of star-branched poly (ε-caprolactone)s with the variation in arm numbers and lengths

Jeongsoo Choi, In-Ki Kim, Seung-Yeop Kwak*

Hyperstructured Organic Materials Research Center (HOMRC), and School of Materials Science and Engineering, Seoul National University, San 56-1, Shinlim-dong, Kwanak-ku, Seoul 151-744, South Korea

Received 12 June 2005; received in revised form 19 August 2005; accepted 22 August 2005
Available online 13 September 2005

Abstract

A series of star-branched poly(ε-caprolactone)s (SPCLs) was synthesized with structural variation of the arm numbers and lengths through ring-opening polymerization under bulk condition. Arm numbers were varied to be 3, 4, and 6 by using multifunctional initiating cores such as trimethylol propane, pentaerythritol, and dipentaerythritol, respectively. The lengths of the poly(ε-caprolactone) arms were varied by controlling the molar ratio of monomer-to-initiating hydroxyl group molar ratio ($[CL]_0/[-OH]_0 = 5$, 10, 15). Molecular weights were determined by both ^{1}H NMR end-group analysis and MALDI-TOF mass spectrometry, which gave reasonably consistent values. On the contrary, the GPC method failed to give accurate values of molecular weight of SPCLs due to the discrepancy with the linear standard. The branching architecture of SPCLs was evaluated by the branching ratio, g, which is the ratio of the mean-square radius of SPCL to that of liner counterpart, linear poly(ε-caprolactone) (LPCL), which is of the same chemistry and having the same molecular weight. The radii of gyration of SPCLs and LPCLs were determined using small-angle X-ray scattering (SAXS) from the initial slopes of Zimm plots, represented as $1/I(q)$ vs q^2 with $I(q)$ and q being the scattered intensity and scattering vector, respectively. The g values were observed to decrease with increasing arm numbers, indicating more compact molecular structure for SPCLs with higher arm numbers, while no such effect was observed for arm length variation. Thermal properties as well as the degree of crystallinity of SPCLs were found to be also dependent on structural variations. The melting points and the degradation temperatures were observed to increase with increasing arm lengths but with constant arm number. On the other hand, arm number variation with constant arm length gave no such changes to the thermal transitions of SPCLs. However, for the SPCLs with equivalent molecular weights, the degree of crystallinity was found to decrease with increasing arm numbers.
© 2005 Published by Elsevier Ltd.

Keywords: Star-polymer; Poly(ε-caprolactone); Architecture

1. Introduction

Macromolecules with complex molecular architectures have drawn great attention among many scientists and engineers in relations to the functional materials for nanoscale application as new and/or improved material properties can be achieved by altering their specific molecular architecture [1,2]. One such example in this context is the dendritic macromolecules, which are largely classified into dendrimers, hyperbranched polymers, and multi-arm star-branched polymers [3,4]. Dendrimers are generally synthesized by step-by-step reaction based on divergent or convergent methods, which result in molecules with a well-defined monodisperse structure [1,5–7]. However, the tedious and multi-step synthetic process of most dendrimers limits them from being applied in large-scale production. On the other hand, hyperbranched polymers are more advantageous since they can be easily synthesized through a one-step polymerization of AB_x ($x \geq 2$) monomers [8,9]. Due to their highly functionalized globular architectures, hyperbranched polymers exhibit different properties from those of their linear counterpart such as less entanglement in the solid state [1], high solubility in various solvents, low melt viscosity [10–12], and fast molecular motion [13,14]. However, there has been report of few methods of precisely controlling the architecture to impose the tailor-made properties to hyperbranched polymers for their specific application. Lastly, star-branched polymers, which can be distinguished by the structure containing

* Corresponding author. Tel.: +82 2 880 8365; fax: +82 2 885 1748.
E-mail address: sykwak@snu.ac.kr (S.-Y. Kwak).

0032-3861/$ - see front matter © 2005 Published by Elsevier Ltd.
doi:10.1016/j.polymer.2005.08.057

several linear arms of similar molecular weight that emanate from a central core, represent a special case of branched polymers. Like dendrimers, they can possess a globular architecture and have defined inner and peripheral groups, which imparts unique properties to the molecules [15,16]. At the same time, similarly to hyperbranched polymers, their synthesis can be accomplished expeditiously, which makes them promising candidates for practical application [17,18]. Moreover, owing to the progress in controlled polymerization techniques, star-branched polymers can be easily prepared with narrow molecular weight distribution and with predictable lengths and numbers of arms under modest condition [19–21].

Recently, the ring-opening polymerization (ROP) methods have been increasingly adopted for preparing dendritic macromolecules, including dendritic [22–24], hyperbranched [25,26], and multi-arm star-branched polymers [18,27–29] with well-defined building blocks, controlled molecular weights, and narrow molecular weight distributions. Hedrick et al. developed a novel synthetic approach to hyperbranched aliphatic polyesters with a range of molecular architectural variation such as different lengths of linear backbone segments in each building block, the size of macromolecules, and the total molecular weights by means of ROP of ε-caprolactone [25,26]. They, then, conducted investigation on the syntheses of dendrimer-like star polymers from multi hydroxyl-functional 2,2-bis(hydroxymethyl)propionic acid (bis-MPA) derivatives as core molecules [22] and further on the amphiphilic copolymers with poly(methyl methacrylates)s by adopting atom transfer radical polymerization [23,24]. The other types of star-branched poly(ε-caprolactone)s have been prepared from simple multifunctional alcohols such as trimethylolpropane and pentaerythritol or from glycerol [18,27–29]. However,

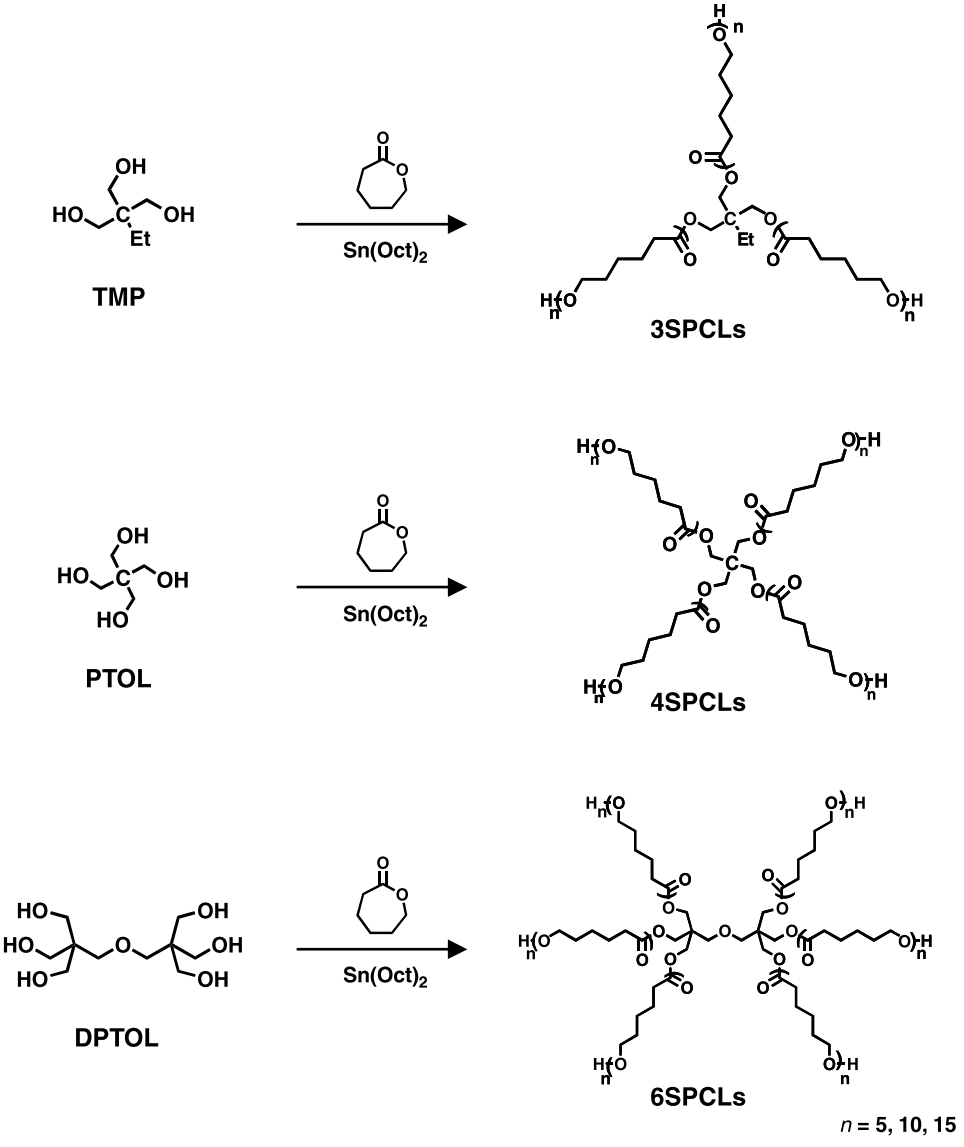

Scheme 1.

the architectural characteristics as well as the correlation between architecture and properties of these hyper- and/or star-branched poly(ε-caprolactone)s have been much less pervasive than other types of dendritic macromolecules. Moreover, previous researches had focused mostly on synthetic variation of the composition of building blocks.

Recently, we reported on the common degree of branching to describe the branching architecture could not be achieved for hyperbranched poly(ε-caprolactone)s by the conventional spectroscopic methods. In connection to this, we proposed an alternative tool for architectural characterization by means of comparing molecular dimension of branched molecule to that of linear counterpart [30]. In addition, we reported the effects of the branching architecture on the thermal properties [30], crystallization kinetics [31], and molecular motion characteristics [32] of hyperbranched poly(ε-caprolactone)s prepared with architectural variations. From this, we extended our studies to the syntheses of star-branched poly(ε-caprolactone)s with the architectural variation on arm numbers and lengths and to the characterization of effects on branching, thermal properties and crystallinity.

In this paper, we will describe the syntheses of a series of star-branched poly(ε-caprolactone)s (SPCLs) possessing architectural variations on arm numbers and lengths by means of ROP of ε-caprolactone. Chemical structures of synthesized SPCLs were confirmed by both ^{1}H and ^{13}C NMR spectroscopy, and the absolute molecular weights were determined by end-group analysis and matrix-assisted laser desorption/ionization time-of-flight (MALDI-TOF) mass spectrometry. The branching architectures were compared by the branching ratio values estimated from the ratio of the mean-square radius of gyration of a given SPCL to that of its linear counterpart. Here, small-angle X-ray scattering (SAXS) was utilized for determining the radii of gyration. The thermal properties and the degree of crystallinity were evaluated using differential scanning calorimetry (DSC) and by performing a thermogravimetric analysis (TGA).

2. Experimental section

2.1. Materials

Trimethylol propane (TMP, 98%), pentaerythritol (PTOL, 99%), dipentaerythritol (DPTOL), tin (II) 2-ethylhexanoate ($Sn(Oct)_2$, 99%) and ethanol (EtOH, 99%) were purchased from Aldrich Chemical and used without further purification except DPTOL which was dried at 180 °C for several hours. ε-Caprolactone (CL, Aldrich, 99%) was dried over CaH_2 for 24 h, distilled under reduced pressure, and stored over activated 4 Å molecular sieves. Tetrahydrofuran (THF, 99%) and methanol (MeOH, 99%) were purchased from Daejung Chemicals and Metals (Korea) and used as received.

2.2. Synthesis

2.2.1. Star-branched poly(ε-caprolactone)s

Star-branched poly(ε-caprolactone)s (SPCLs) were prepared by ring-opening polymerization of CL which was initiated with multifunctional initiating cores in the presence of catalytic amount of $Sn(Oct)_2$. Variation in the number of arms was accomplished by using different initiating core molecules having 3 (TMP), 4 (PTOL), and 6 (DPTOL) hydroxyl groups (Scheme 1). On the other hand, the arm lengths were varied by controlling monomer-to-hydroxyl group molar ratio, which was $[CL]_0/[-OH]_0 = 5$, 10, and 15 in the present study.

The average degrees of polymerization of CL onto each hydroxyl group, n in Scheme 1, were found to be perfectly controlled by this method, which we will discuss in detail in the later section. The basic reaction procedure of the SPCLs is as follows. Five hundred millimole of CL and a certain amount of multifunctional core were put into the reaction flask, which was followed by the three repeated session of evacuation and argon purging processes. The flask was then immersed into an oil bath stabilized at 110 °C with vigorous stirring to form a homogeneous mixture, to which the catalytic amount of $Sn(Oct)_2$ was added. The evacuating and argon purging processes were repeated again and the polymerization was allowed to proceed at 110 °C under dry argon atmosphere for 24 h. The reaction mixture was then cooled to room temperature, dissolved in THF, and poured dropwise into an excess of cold methanol. The precipitates were washed with methanol for several times and dried at room temperature in a vacuum. On the basis of the different arm numbers (m) and arm lengths (n), the resulting SPCLs of the present study were accordingly designated as mSPCL-n where $m = 3$, 4, 6, and $n = 5$, 10, 15, respectively. Yield: 85–96%.

2.2.2. Linear poly(ε-caprolactone)s

Linear poly(ε-caprolactone)s (LPCLs) were prepared as the linear counterparts to the synthesized SPCLs having the same chemistry as well as similar molecular weights. The general procedures for the syntheses of LPCLs were the same as those of the SPCLs, except that EtOH which was used as an initiator instead of multifunctional cores and monomer-to-initiator molar ratio, the targeted degree of polymerization of CL, was varied to be $[CL]_0/[-OH]_0 = 17$, 32, 42, and 63, respectively, in order to control the molecular weights of the resulting LPCLs. Synthesized LPCLs were named as LPCL-17, -32, -42, and -63 according to the respective targeted degree of polymerization. Yield: 95–98%.

2.3. General characterization

2.3.1. Nuclear magnetic resonance (NMR) spectroscopy

Chemical structures of synthesized SPCLs as well as those of LPCLs were characterized via ^{1}H and ^{13}C NMR

spectroscopy. Both ^{1}H and ^{13}C NMR spectra were acquired on a Bruker Avance DPX-300 (300 MHz for ^{1}H and 75 MHz for ^{13}C) spectrometer using $CDCl_3$ as solvent and tetramethylsilane (TMS) as an internal standard. ^{1}H NMR spectra were also analyzed to determine the average degree of polymerization of CL onto each hydroxyl group of core molecules $\langle DP_{CL} \rangle$, and consequently the number-average molecular weights of the polymers, $M_{n,NMR}$. More detailed explanation about the methods for determining the values of $\langle DP_{CL} \rangle$ and $M_{n,NMR}$ will be shown in Section 3.

2.3.2. Gel permeation chromatography (GPC)

The GPC experiments were performed using a waters chromatograph system consisting of Waters 1515 HPLC pump, 2414 refractive index detector, and a set of ultrastyragel columns (HR2 + HR4 + HR5). Polystyrene of known molecular weights was used as calibration standard, and reagent-grade THF was used as mobile phase eluting at a flow rate of 1.0 mL/min. A 100 μL sample of a 0.1 mg/mL solution in THF, which was filtered through a 0.2 μm Whattman filter prior to use, was injected for all measurements.

2.3.3. Matrix-assisted laser desorption/ionization time-of-flight (MALDI-TOF) mass spectrometry

MALDI-TOF mass spectrometric measurements were carried out on a PerSeptive Biosystems-Voyager-DE STR spectrometer equipped with a nitrogen laser (337 nm, 3 ns pulse width) in deflected mode. The accelerating voltage was fixed at 20 kV, the grid voltage 80%, and the guide wire voltage 0.1%. All samples were dissolved in THF, and matrix solution was prepared as dithranol/THF (C = 10 mg/mL). A 2 μL sample of a 1:1 mixture of sample/matrix solution was loaded into a single well of a teflon-coated stainless steel plate and dried before being inserted into the vacuum chamber of the MALDI instrument. Each MALDI spectrum was the average of 256 laser shots accumulation.

2.3.4. Small-angle X-ray scattering (SAXS)

The radii of gyration, R_g's, of the SPCLs and their linear counterparts, LPCLs, were determined by SAXS. The SAXS intensity distribution, $I(q)$, was measured as a function of scattering vector, q, with a rotating-anode X-ray generator (Bruker AXS Nanostar) operated at 40 kV and 35 mA, of which X-ray source was a monochromatized Cu Kα (λ = 1.54 Å) radiation. The scattering angle range between 0.1 and 2° and the sample-to-detector distance of 106 cm was employed, respectively. Dilute solution samples of concentration being 1 mg/mL in THF were injected into glass capillary loaded in liquid sample holder frame. The background correction was carried out to yield absolute scattering intensity from the sample by measuring incoherent scattering from a cell with pure THF and subtracting it from the raw intensity data. The R_g values were estimated by curve fitting of the reciprocal plots of $I(q)$ as a function of q using the Zimm particle scattering function, which will be described in detail in following section.

2.3.5. Differential scanning calorimetry (DSC) and thermogravimetric analysis (TGA)

Melting temperature, T_m, and the heat of fusion, ΔH_m, for the SPCLs were measured by DSC with a TA Instruments DSC 2920 at a heating rate of 20 °C/min under a nitrogen atmosphere. T_m and ΔH_m were determined from the maximum endothermic peak position and integrating of endothermic area at the second heating run. Thermogravimetric analysis (TGA) was carried out on a TA Instruments TGA 2050 thermal analyzer at a heating rate of 20 °C/min under a nitrogen atmosphere and the masses of samples were approximately 5–10 mg. Thermal degradation stability

Table 1
Synthesis of star-branched poly(ε-caprolactone)s and linear poly(ε-caprolactone)s

Sample	Initiator entry	Hydroxyl functionality	$[CL]_0/[-OH]_0$[a]	$\langle DP_{CL} \rangle$[b]	$M_{n,NMR}$[c]	Yield[d] (%)
3SPCL-5	TMP	3	5	5.6	2100	85
3SPCL-10	TMP	3	10	10.4	3700	94
3SPCL-15	TMP	3	15	15.4	5400	95
4SPCL-5	PTOL	4	5	5.5	2800	86
4SPCL-10	PTOL	4	10	10.6	5100	95
4SPCL-15	PTOL	4	15	15.5	7400	96
6SPCL-5	DPTOP	6	5	5.3	3900	88
6SPCL-10	DPTOP	6	10	10.4	7400	95
6SPCL-15	DPTOP	6	15	15.2	10,700	96
LPCL-17	EtOH	1	17	17.3	2000	95
LPCL-32	EtOH	1	32	31.3	3600	97
LPCL-42	EtOH	1	42	43.7	5000	98
LPCL-63	EtOH	1	63	61.9	7100	97

[a] Molar ratio of CL monomer-to-initiating hydroxyl group.
[b] Average degree of polymerization of oligo(ε-caprolactone) arm segments of SPCLs.
[c] Number-average molecular weight determined by ^{1}H NMR.
[d] Insoluble part in cold methanol.

of the SPCLs was evaluated using the temperature of 10% weight loss of the polymers, T_{d10}.

3. Results and discussion

3.1. Synthesis of star-branched poly(ε-caprolactone)s

Synthetic routes to the star-branched poly(ε-caprolactone)s (SPCLs) with the variation in both arm numbers and lengths are well represented in Scheme 1. As can be seen in Scheme 1, the arm number variation was realized by using different multifunctional cores having 3, 4, and 6 hydroxyl groups which were TMP, PTOL, and DPTOL, respectively. Ring-opening polymerizations of CL with variable molar ratios of CL-to-initiation hydroxyl group in multifunctional cores ($[CL]_0/[-OH]_0 = 5$, 10, and 15) enabled a controlled variation of arm length of the resulting SPCLs.

Table 1 summarizes the conditions for preparing SPCLs and LPCLs. The chemical structures of the resulting SPCLs were confirmed from both ^{1}H NMR and ^{13}C NMR spectra as shown in Fig. 1(a) and (b), although these spectra for 4SPCL-10 are only shown here as examples. From ^{1}H and ^{13}C NMR spectra for the synthesized SPCLs, we could easily see that $Sn(Oct)_2$ catalyzed ring-opening polymerization of CL was successful in producing SPCLs. In addition, ^{1}H NMR spectra of SPCLs and LPCLs were also analyzed to determine the average degree of polymerization of oligo(ε-caprolactone) arm segments of SPCLs, $\langle DP_{CL} \rangle$, and the number-average molecular weights, $M_{n,NMR}$.

As indicated in Fig. 1(a), the peak assigned to the chain ends (*a*, $-CH_2OH$, δ 3.65) and the peak assigned to the repeating methylene units (*c*, $-COCH_2$, δ 2.31) in poly(ε-caprolactone) segments were quite distinguishable for ^{1}H NMR spectra of all SPCLs and LPCLs. Therefore, the $\langle DP_{CL} \rangle$ values, which are the lengths of arms in the case of SPCLs or the lengths of linear polymer chain in the case of LPCLs, could be easily calculated from the ratios of the integrated area of the peak *a* to that of the peak *c*.

As listed in Table 1, the calculated $\langle DP_{CL} \rangle$ values for SPCLs as well as those for LPCLs were found to be in good agreement with those of the targeted values, which are solely predictable from the $[CL]_0/[-OH]_0$ ratios. The initiator efficiencies can be calculated from the ratios of the targeted to the experimental values of DP. Among the initiators used in this study, TMP showed relatively low efficiencies for the syntheses of the SPCLs with short arms (89–94%), whereas the other initiators showed high efficiencies (96–99%). Also, the polymerization yields estimated from the insoluble part in cold MeOH were found to be relatively low for the SPCLs with short arms (85–88%). These might be resulted from the relatively low reagent purity and non-precipitated low molecular weight byproducts, respectively. The number-average molecular

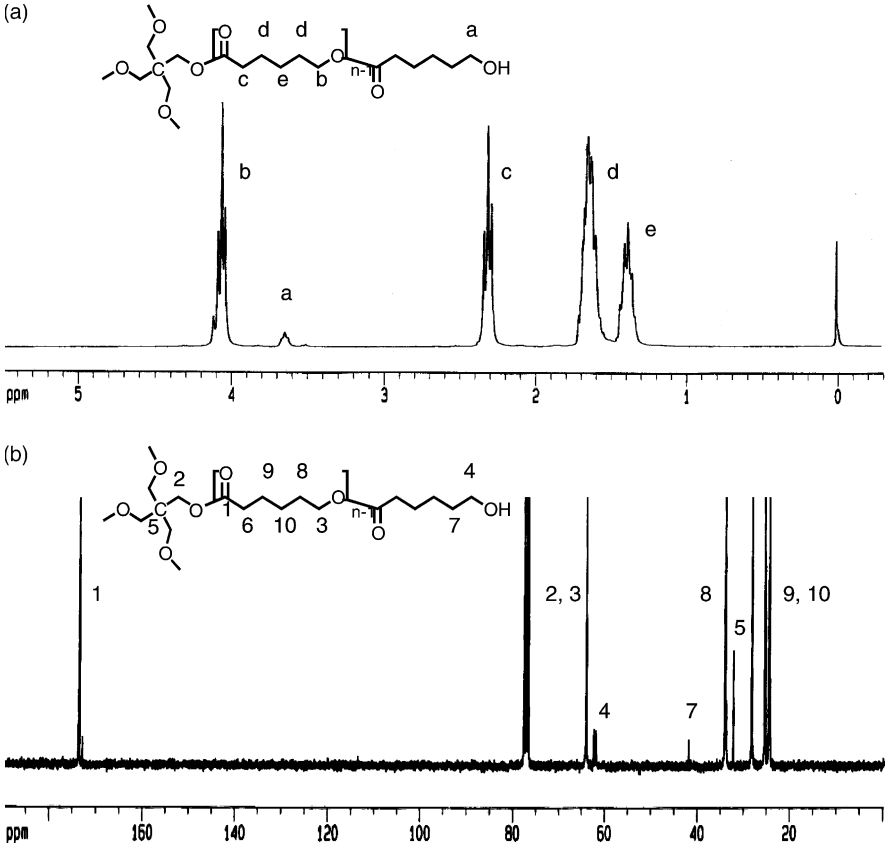

Fig. 1. (a) ^{1}H and (b) ^{13}C NMR spectra of 4SPCL-10.

weights of the SPCLs and LPCLs, $M_{n,NMR}$, were calculated from the following equation (Table 1):

$$M_{n,NMR} = MW_{Ini} + MW_{CL} \times \langle DP_{CL} \rangle \times (\text{arm number}) \quad (1)$$

where MW_{Ini} is the molecular weight of initiating species (TMP, PTOL, and DPTOL for SPCLs and EtOH for LPCLs), and MW_{CL} is that of CL.

Fig. 2 shows the plot of estimated $M_{n,NMR}$ vs molar ratio of $[CL]_0/[-OH]_0$, in which $M_{n,NMR}$ of SPCLs are shown to increase linearly with $[CL]_0/[-OH]_0$ molar ratio. In addition, we found that LPCLs were successfully obtained with the targeted degrees of polymerization and thus with the desired average molecular weights being similar to their corresponding star-branched counterparts.

Conventional gel permeation chromatography (GPC) calibrated by polystyrene standard samples of known molecular weights and narrow distributions was conducted for SPCLs to compare with the results from the ^{1}H NMR end-group analyses. As exemplary shown in Fig. 3 for 4SPCLs, GPC gave smooth and monomodal chromatograms for all SPCLs. Also, it was clearly observed that the chromatograms of SPCLs were shifted toward lower retention volume area as the arm lengths increased as follows: 4SPCL-5 > 4SPCL-10 > 4SPCL-15. Average molecular weights and molecular weight distributions for all SPCLs were estimated from the standard calibration curve and are summarized in Table 2.

As shown in Table 2, the number-average molecular weights obtained from GPC, $M_{n,GPC}$, were somewhat lower than those from ^{1}H NMR end-group analyses, which usually occurs when characterizing the molecular weights of branched polymers with GPC. This is generally ascribed to the inevitable decrease in the hydrodynamic volume imposed by branching [33], which in turn exceeds the relative discrepancy with the polystyrene standards [34]. It had been previously reported that molecular weights for hyperbranched poly(ε-caprolactone)s were detected to

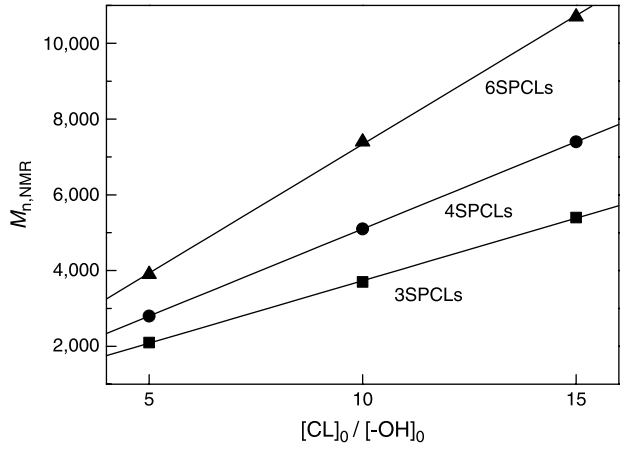

Fig. 2. Dependence of M_n on the molar ratio of $[CL]_0/[-OH]_0$ with TMP (3SPCLs), PTOL (4SPCLs), and DPTOL (6SPCLs) multifunctional initiators.

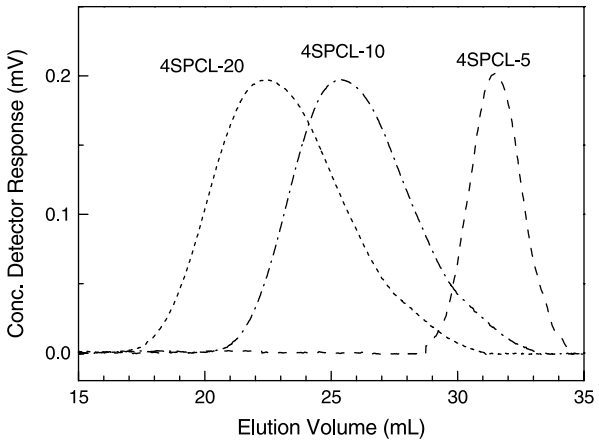

Fig. 3. GPC chromatograms of 4SPCLs with different arm lengths.

deviate toward lower values compared to their absolute ones when characterized by conventional GPC [30]. Thus, in this study, where we deal with the matrix-assisted laser desorption/ionization time-of-flight (MALDI-TOF) mass spectrometry, we experimented on an alternative approach for determining the absolute molecular weights for SPCLs.

Fig. 4 depicts the MALDI-TOF mass spectra for 4SPCLs. Peaks with the highest intensity are attributed to the sodium ion adducts, which are the results of the cationization by arbitrary sodium impurities in the samples [35]. The mass difference between each adjacent peak, Δm, is 114 Da, which corresponds well with the mass of the CL repeating unit of the chain segments in SPCLs. The spectrum of 4SPCL-5 contains peaks extending from approximately $m/z = 1500$–4000. Arm length variations made by controlled increase in the $[CL]_0/[-OH]_0$ from 5 to 10 and 15, respectively, shifted the whole mass distribution curves to higher molecular weights while the distribution shape showed no significant changes. As can be seen from Figs. 3 and 4, the distributions are narrower for the SPCLs with short arms compared to those for the SPCLs with longer arms, which might be resulted from the loss of

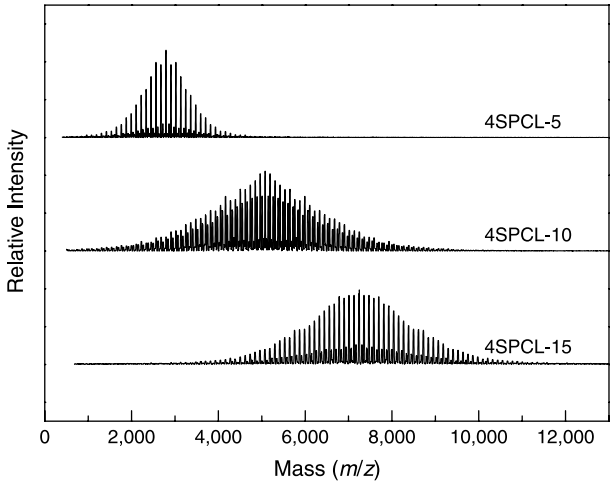

Fig. 4. MALDI-TOF mass spectra of 4SPCLs with different arm lengths.

Table 2
Molecular weight and molecular weight distribution of star-branched poly(ε-caprolactone)s determined by ^{1}H NMR end-group analysis, GPC, and MALDI-TOF mass spectrometry

Sample	$M_{n,NMR}$	GPC		MALDI-TOF	
		$M_{n,GPC}$	M_w/M_n	$M_{n,MALDI}$	M_w/M_n
3SPCL-5	2100	2100	1.18	2000	1.08
3SPCL-10	3700	3100	1.34	3600	1.17
3SPCL-15	5400	4900	1.42	5300	1.22
4SPCL-5	2800	2200	1.19	2800	1.09
4SPCL-10	5100	4100	1.40	5100	1.17
4SPCL-15	7400	5200	1.46	7200	1.18
6SPCL-5	3900	2800	1.26	3800	1.12
6SPCL-10	7400	5000	1.37	7400	1.17
6SPCL-15	10,700	6400	1.50	N/A	N/A

the low molecular weight byproducts during the precipitation in cold MeOH.

The average molecular weights and molecular weight distributions for SPCLs were derived from the MALDI-TOF mass spectra and listed in Table 2. For the SPCLs, the number-average molecular weights determined by the MALDI-TOF mass spectrometry, $M_{n,MALDI}$, were found to be in good agreement with those from the ^{1}H NMR end-group analyses, $M_{n,NMR}$. This shows that, unlike conventional GPC, both MALDI-TOF mass spectrometry and ^{1}H NMR end-group analysis can be utilized to determine absolute molecular weights of SPCLs. On the contrary, molecular weight distributions measured by MALDI-TOF were observed to be generally narrower than those determined from GPC measurements as listed in Table 2. This had already been reported by Müllen et al. [36]. The desorption/ionization of high molecular weight polymers require higher laser power than do low molecular weight polymers. Therefore, for polydisperse polymer samples, this effect may produce smaller peak areas for the high mass components and accordingly produce narrower distribution in MALDI-TOF analysis [35,36].

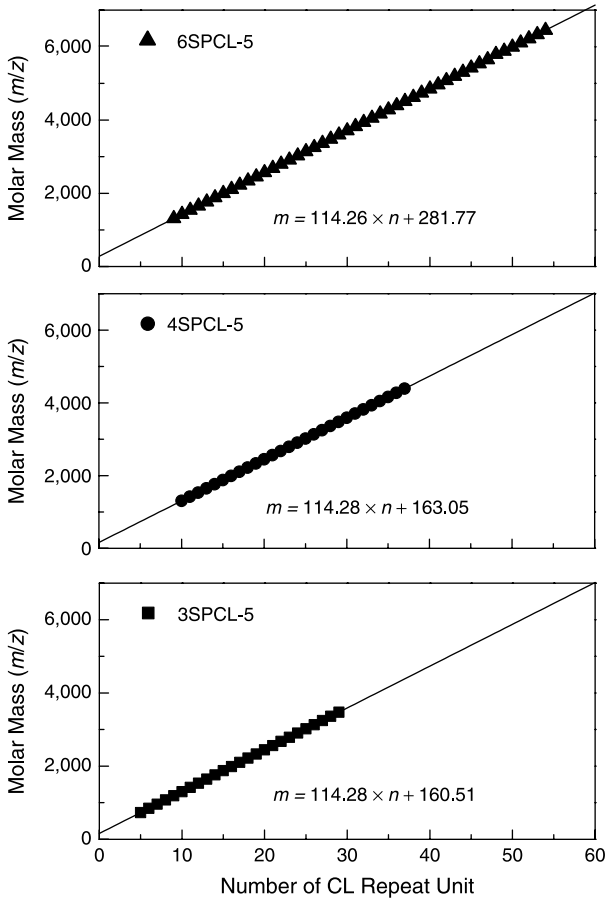

Fig. 5. Plot of m/z values from MALDI-TOF vs number of CL repeat unit for 3SPCL-5, 4SPCL-5, and 6SPCL-5.

Another advantage of the MALDI-TOF mass spectrometry is its ability to provide information of polymer end groups. By considering the calculated mass and the experimental mass of a single oligomer, the functional groups of both polymer chain ends can be analyzed. The calculated mass $m(n)$ of single peak of the molecular weight distribution curve is a linear function of the number of repeat unit n as expressed as follows [35]:

$$m(n) = n \times m_{monomer} + m_{end\ groups} + m_{cation} \quad (2)$$

where $m_{monomer}$ is the mass of the monomer, $m_{end\ groups}$ is the residue mass of both end groups, and m_{cation} is the mass of the alkali cation being Na^+ in this study. Fig. 5 shows a correlation of the mass (m/z) measured by MALDI-TOF for 3SPCLs, 4SPCLs, and 6SPCLs as a function of the number of CL repeat units. The slopes of the fitted lines for SPCLs with three different arm numbers are very close to the actual mass of CL monomer (114.14 Da). The values for three intercepts (160.51, 163.05, and 281.77) are fairly close to the expected masses, which were estimated from the sum of the masses of multifunctional cores used (TMP, PTOL, DPTOL) and the mass of the cation, of 157.18, 159.15, and 277.28 Da, respectively.

3.2. Molecular dimension and branching ratio

In order to characterize the effect of the branching architecture on molecular dimension, the branching ratio, g, was estimated from the ratio of the mean-square radii of

gyration between a given star-branched molecule and its linear counterpart with the same chemistry and similar molecular weight as follows [37]:

$$g = \frac{\langle R_g^2 \rangle_{branched}}{\langle R_g^2 \rangle_{linear}} \tag{3}$$

where $\langle R_g^2 \rangle_{branched}$ and $\langle R_g^2 \rangle_{linear}$ denote the mean-square radius of gyration of star-branched molecule and that of linear counterpart, respectively. It should be noted that the parameter g is always <1, and decreases with increase in degree of branching, because branched molecules occupy less volume in solution than linear polymers of the same molecular weight [33,38]. The radii of gyration for SPCLs as well as those for their linear counterpart were determined by small-angle X-ray scattering (SAXS). The scattering curves obtained from polymer solutions, after correcting for instrumental effects, generally consist of scattering contributions from the single particle scattering, the molecular size and the shape of a single particle as well as the interparticle interference. Therefore, the scattering from a group of particles can be expressed as

$$I(q) = k \times N \times P(q) \times S(q) \tag{4}$$

where $I(q)$ is the experimental scattered intensity, q is the scattering vector, k is an electron density contrast factor, N is the number of particles, $P(q)$ is the single particle scattering function, and $S(q)$ is the interparticle scattering function [39]. However, assuming that the sample solutions of the HPCLs and LPCL ($C_{polymer}$ = 1 mg/mL) are very dilute and in a non-interacting system, the interparticle scattering effect can be ignored (i.e. $S(q) \rightarrow 1$). Therefore, Eq. (4) can be simplified as a function of only model particle scattering function, $P(R_g,q)$, which enables us to extract the R_g values from the scattering curves by performing a weighted non-linear, least-square that fit the scattering curves over the q range, $[q_{min}, q_{max}]$ [39]:

$$I(q) = A \times P(R_g, q) + B, \quad [q_{min}, q_{max}] \tag{5}$$

The most common model particle scattering functions are those suggested by Zimm [40] and Guinier [41], which are shown below:

$$P_{Zimm}(R_g, q) = \frac{1}{(1 + (q^2 R_g^2/3))} \tag{6}$$

$$P_{Guinier}(R_g, q) = \exp\left(-\frac{q^2 R_g^2}{3}\right) \tag{7}$$

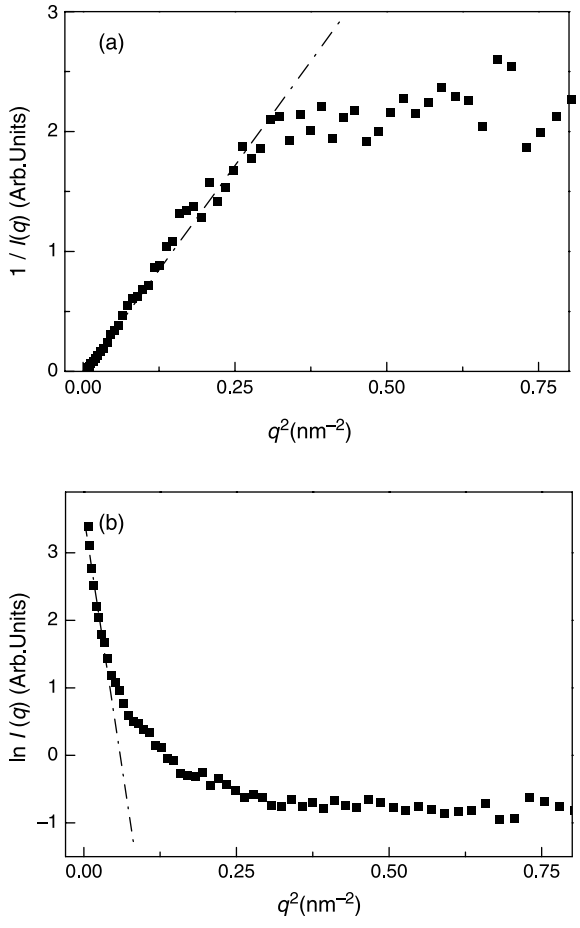

Fig. 6. SAXS scattering curves of 6SPCL-10 plotted by (a) Zimm and (b) Guinier method. The dashed lines indicate the weighted linear least-square fits in the selected linear regions at low-q regime.

Fig. 6 shows the typical scattering curves for the SPCLs observed by SAXS. It should be noted that only those for 6SPCL-10 are shown here in terms of the (a) Zimm plot being $1/I(q)$ vs q^2 and the (b) Guinier plot being $\ln I(q)$ vs q^2, respectively. For the Zimm plot in Fig. 6(a), 6SPCL-10 appeared linear over a relatively large q range, while 6SPCL-10 for the Guinier plot had an extremely strong curvature near the origin as shown in Fig. 6(b). Similar tendency that SAXS curve fitting by P_{zimm} was more accurate than fitting by $P_{Guinier}$, has been reported for the case of hyperbranched poly(ε-caprolactone)s [30]. In order to elucidate the effects of arm numbers and lengths on molecular dimension, respectively, the R_g values for 4SPCLs, SPCL-10's, and their counterparts were determined, and the results are summarized in Table 3 along with calculated g values.

As shown in Fig. 7, for the SPCLs with the same arm number, the g values remained almost constant (g = ca. 0.8). This indicates that the segment density was not significantly varied when the arm length was increased. However, the g values, for SPCLs having the same arm length, were observed to decrease as arm number is increased. This indicates that more branching points resulted in more compactly packed volume in the solution.

3.3. Thermal properties

Thermal properties of SPCLs were characterized using both DSC and TGA. Fig. 8(a) shows the DSC thermograms

Table 3
Radii of gyration of star-branched poly(ε-caprolactone)s and their linear counterparts, and calculated values of branching ratio

Star-branched			Linear counterpart			g
Sample	$M_{n,NMR}$	R_g (Å)	Sample	$M_{n,NMR}$	R_g (Å)	
4SPCL-5	2800	41.4	LPCL-17	2000	46.0	0.81
4SPCL-10	5100	42.1	LPCL-42	5000	47.1	0.80
4SPCL-15	7400	44.27	LPCL-63	7100	49.8	0.79
3SPCL-10	3700	43.9	LPCL-32	3600	46.5	0.89
6SPCL-10	7400	42.7	LPCL-63	7100	49.8	0.74

of 4SPCLs with various arm lengths appearing sharp melting transition peaks, which are seen shift toward a higher temperature region as arm length increase. As shown in Fig. 8(b), the melting temperatures, T_m, for SPCLs of the same arm numbers are seen to be fairly affected by arm length variation, which is assumed to be due to the presence of longer linear chains possibly facilitating the ordered chain packing to crystallize more efficiently [42]. At the same time, the effect of arm numbers on the T_m for SPCLs of the same arm length was shown to be negligible. The T_m and melting enthalpies, ΔH_m, for SPCLs are listed in Table 4. The degree of crystallinity, X_c, of SPCLs were calculated as follows:

$$X_c(\%) = \frac{\Delta H_m}{\Delta H_m^0} \times 100 \quad (8)$$

where ΔH_m is the apparent enthalpy of melting for each SPCL and ΔH_m^0 is the extrapolated value of enthalpy corresponding to the melting of a 100% crystalline poly(ε-caprolactone), which was previously reported as 136.4 J/g [43].

As listed in Table 4, the X_c for SPCLs of the same arm number was increased with increasing arm length. However, for SPCLs of the same arm length, the effect of increasing arm numbers on the X_c was observed to be negligible, which is regarded to be due to the competing effects of increased molecular weight and branching. In order to investigate the sole effect of branching on the X_c, it is necessary to compare the X_c for SPCLs of similar molecular weight with different arm numbers. Here, it is worthy to note that the X_c for SPCLs of similar molecular weight was decreased for the larger arm numbers, i.e. 3SPCL-15 > 4SPCL-10, 3SPCL-10 > 6SPCL-5, and 4SPCL-15 > 6SPCL-10, which is due to a larger number of free chain ends disrupting the orderly fold pattern of the crystal [28]. This is well reflected in Fig. 9 where the X_c for SPCLs are illustrated as a function of total molecular weights (Table 4).

Fig. 10 depicts the TGA thermograms of 4SPCLs with various arm lengths, in which the temperature of 10% weight loss, T_{d10}, of 4SPCLs are seen to shift toward a higher temperature region as the arm length was increased.

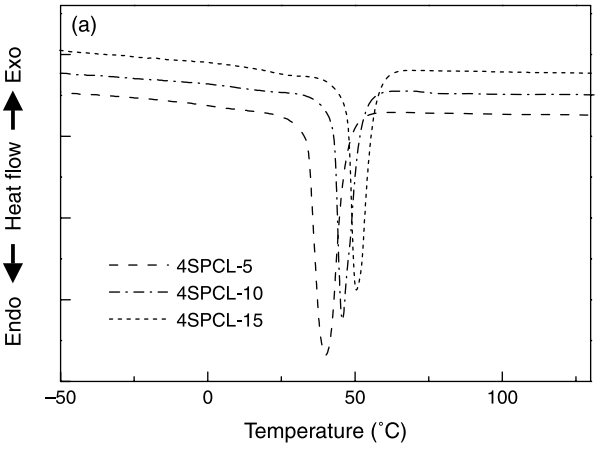

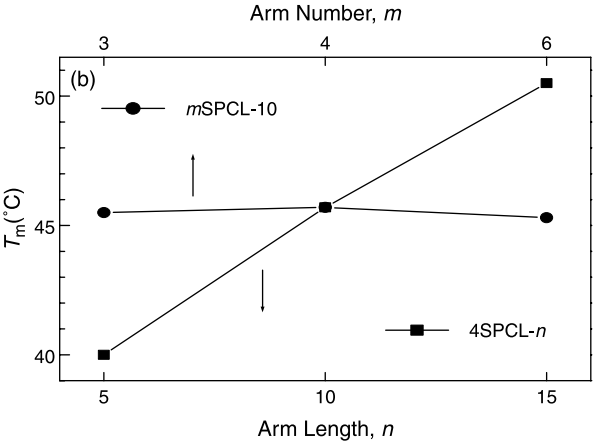

Fig. 8. (a) DSC thermograms of 4SPCLs and (b) dependence of T_m on arm lengths and numbers.

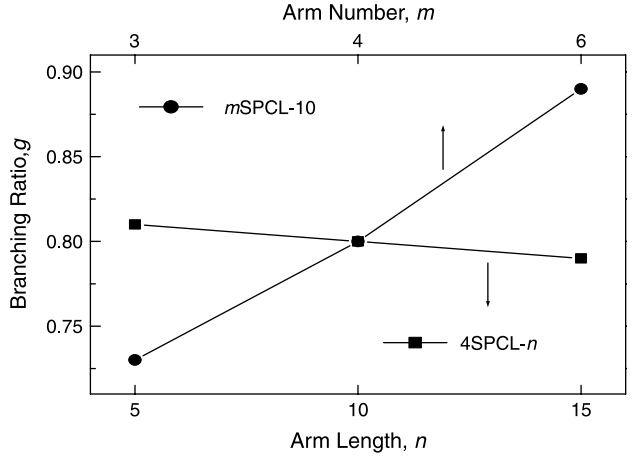

Fig. 7. Dependence of branching ratio on arm lengths of 4SPCLs (bottom axis) and on arm numbers of SPCL-10's (top axis).

Table 4
Melting point (T_m), enthalpy of fusion (ΔH_m), degree of crystallinity (X_c), and degradation temperatures (T_{d10}) of star-branched poly(ε-caprolactone)s

Sample	T_m (°C)	ΔH_m (J/g)	X_c (%)	T_{d10} (°C)
3SPCL-5	37.9	72.2	52.9	319
3SPCL-10	45.5	74.5	54.6	322
3SPCL-15	50.2	76.6	56.1	326
4SPCL-5	40.0	71.2	52.2	320
4SPCL-10	45.7	73.7	54.1	323
4SPCL-15	50.5	75.7	55.5	326
6SPCL-5	40.7	68.9	50.5	320
6SPCL-10	45.3	73.2	53.6	322
6SPCL-15	51.2	75.1	55.1	327

Thermal degradation of poly(ε-caprolactone) has been reported to involve an unzipping depolymerization from the hydroxyl end of the polymer chain [44,45]. Considering this thermal degradation mechanism for poly(ε-caprolactone), increase of T_{d10} of SPCLs with longer arms are believed to be attributed to the lower number of polymer chain ends. On the contrary, T_{d10} for SPCLs of similar molecular weight were found to decrease as arm numbers increased, i.e. 3SPCL-15 > 4SPCL-10, 3SPCL-10 > 6SPCL-5, and 4SPCL-15 > 6SPCL-10, which may result in the higher number of chain ends and consequently resulting in the acceleration of unzipping degradation.

4. Conclusions

1. A series of star-branched poly(ε-caprolactone)s (SPCLs) was successfully synthesized with structural variation of arm numbers and length through ring-opening polymerization of CL in the presence of $Sn(Oct)_2$ catalyst. Arm number was varied by using different multifunctional cores having 3 (TMP), 4 (PTOL), and 6 (DPTOL) hydroxyl groups. Arm length was varied by controlling the molar ratio of $[CL]_0/[–OH]_0$ being 5, 10, and 15. Structural variations among SPCLs were verified to be precisely controlled as evidenced by ^1H and ^{13}C NMR spectra. The absolute values of molecular weight were obtained by both ^1H NMR end-group analysis and MALDI-TOF mass spectrometry, of which results were reasonably consistent. In addition, the M_n of SPCLs were found to be a linear function of molar ratio of $[CL]_0/[–OH]_0$. On the contrary, the GPC method failed to give accurate molecular weight information of SPCLs due to the discrepancy with the linear standard.
2. The molecular dimension of SPCLs was estimated using the radius of gyration, R_g, determined by SAXS curve fits to the Zimm scattering function. The branching ratio, g, was calculated from the ratio of the mean-square radius of gyration of each SPCL to that of its linear counterpart of the equivalent molecular weight, which was found to be quite instrumental in obtaining a better understanding of the architectural characteristics of SPCLs. In addition, g was observed to be fairly affected by arm number variation; the higher arm numbers, the smaller g values, and thus more compact molecular structure in order of 3SPCL-10 > 4SPCL-10 > 6SPCL-10, while the effect of arm length variation on g of SPCLs was found to be only minimal.
3. We also found the correlative effect of structural variation on the thermal transitions as well as the degree of crystallinity of SPCLs as revealed by DSC and TGA. The T_m was found to increase with increasing arm length, which is explained by the presence of longer linear chains facilitating the ordered chain packing. Similarly, the T_{d10} was observed to be an increasing function of arm length, which is due to the less chain ends in unit volume decelerating unzipping degradation from hydroxyl ends of polymer chain. On the contrary, we did not observe any significant changes in both the T_m and T_{d10} for the SPCLs of the same arm length but with arm number variation. However, for the SPCLs of the equivalent molecular weight, the degree of crystallinity was found to decrease with increasing arm numbers, which might be due to the larger number of

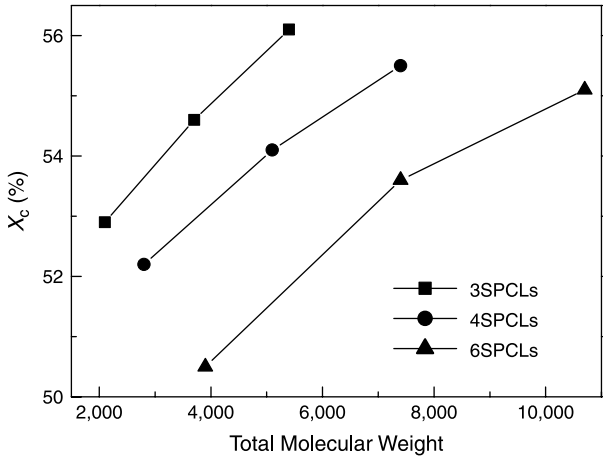

Fig. 9. Degree of crystallinity of SPCLs vs their total molecular weight.

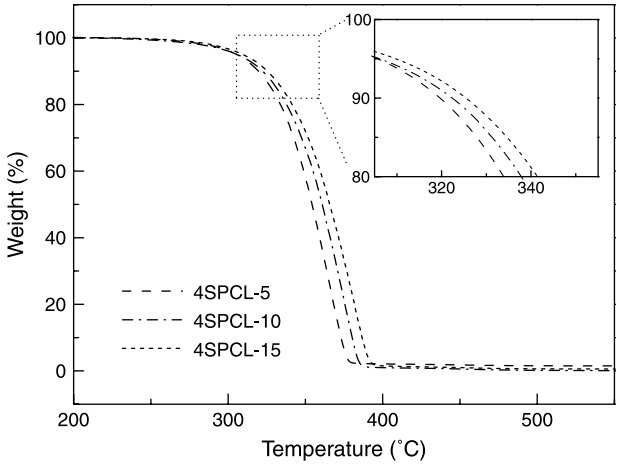

Fig. 10. TGA thermograms of 4SPCLs with different arm lengths.

free chain ends disrupting the orderly fold pattern of the crystals during crystallization.

Acknowledgements

The authors are grateful to the Ministry of Environment, Republic of Korea for their support through Eco-Technopia 21 project.

References

[1] Fréchet JMJ. Science 1994;263:1710.
[2] Hedrick JL, Miller RD, Hawker CJ, Carter KR, Volksen W, Yoon DY, et al. Adv Mater 1998;10:1049.
[3] Gao C, Yan D. Prog Polym Sci 2004;29:183.
[4] Fréchet JMJ, Tomalia DA. Dendrimers and other dendritic polymers. New York: Wiley; 2001.
[5] Newkome G, Moorefield CN, Vogtle F. Dendritic molecules: Concepts, syntheses, perspectives. Weinheim: VCH Publishers; 1996.
[6] Fisher M, Vogtle F. Angew Chem Int Ed Eng 1999;38:885.
[7] Hawker CJ, Malstrom E, Frank CW, Kampf JP. J Am Chem Soc 1997; 119:9903.
[8] Uhrich KE, Hawker CJ, Fréchet JMJ. Macromolecules 1992;25:4583.
[9] Miller TM, Neenan TX, Kwock EW, Stein SM. J Am Chem Soc 1993; 115:356.
[10] Hawker CJ, Farrington PJ, Mckay ME, Wooley KL, Fréchet JMJ. J Am Chem Soc 1995;117:4409.
[11] Mourey TH, Turner SR, Rubinstein M, Fréchet JMJ, Hawker CJ, Wooley KL. Macromolecules 1992;25:2401.
[12] Kim YM, Kim YG. J Ind Eng Chem 1999;5:74.
[13] Kwak S-Y, Lee HY. Macromolecules 2000;33:5536.
[14] Kwak S-Y, Ahn DU. Macromolecules 2000;33:7557.
[15] Mishra MK, Kobayash S, editors. Star and hyperbranched polymers. New York: Dekker; 1999.
[16] Hadichristidis N. J Polym Sci A, Polym Chem 1999;37:857.
[17] Robello DR, André A, McCovick TA, Kraus A, Mourey TH. Macromolecules 2002;35:9334.
[18] Sanda F, Sanada H, Shibasaki Y, Endo T. Macromolecules 2002;35: 680.
[19] Wang J-S, Matyjaszewski K. J Am Chem Soc 1995;117:5614.
[20] Georges MK, Veregin RPN, Kazmaier PM, Hamer GK. Trends Polym Sci 1994;2:66.
[21] Hawker CJ. Acc Chem Res 1997;30:373.
[22] Trollsås M, Hedrick JL. J Am Chem Soc 1998;120:4644.
[23] Hedrick JL, Trollsås M, Hawker CJ, Atthoff B, Claesson H, Heise A, et al. Macromolecules 1998;31:8691.
[24] Stancik CM, Pople JA, Trollsås M, Lindner P, Hedrick JL, Gast AP. Macromolecules 2003;36:5765.
[25] Trollsås M, Atthoff B, Claesson H, Hedrick JL. Macromolecules 1998;31:3439.
[26] Trollsås M, Hedrick JL. Macromolecules 1998;31:4390.
[27] Dong CM, Qui KY, Gu ZW, Feng XD. Macromolecules 2001;34: 4691.
[28] Choi YK, Bae YH, Kim SW. Macromolecules 1998;31:8766.
[29] Lang MD, Wong RP, Chu CC. J Polym Sci A, Polym Chem 2002;40: 1127.
[30] Choi J, Kwak S-Y. Macromolecules 2003;36:8630.
[31] Choi J, Kwak S-Y. Macromolecules 2004;37:3745.
[32] Choi J, Kwak S-Y. Polymer 2004;45:7173.
[33] Podzimek S. J Appl Polym Sci 1994;54:91.
[34] Claesson H, Malmström E, Johansson M, Hult A. Polymer 2002;43: 3511.
[35] Yu D, Vladimirov N, Fréchet JMJ. Macromolecules 1999;32:5186.
[36] Martin K, Spickermann J, Räder JJ, Müllen K. Rapid Commun Mass Spectrom 1996;10:1471.
[37] Zimm BH, Stockmayer WH. J Chem Phys 1949;17:1301.
[38] Roovers J. In: Mark HF, Bikales NM, Overberger CG, Menges G, editors. Encyclopedia of polymer science and engineering, vol. 2, New York: Wiley; 1985.
[39] Prosa TJ, Bauer BJ, Amis EJ, Tomalia DA, Scherrenberg R. J Polym Sci B, Polym Phys 1997;35:2913.
[40] Higgins JS, Benoít HC. Polymers and neutron scattering. Oxford: Claredon Press; 1994.
[41] Guinier A, Fournet G. Small angle scattering of X-rays. New York: Wiley; 1955.
[42] Magnusson H, Malmström E, Hult A, Johansson M. Polymer 2002;43: 301.
[43] Crescenzi V, Manzini G, Calzolari G, Borri C. Eur Polym J 1972;8: 449.
[44] Persenaire O, Alexandre M, Degée P, Dubois P. Biomacromolecules 2001;2:288.
[45] Aoyagi Y, Yamshita K, Doi Y. Polym Degrad Stab 2002;76:53.